Available online at www.sciencedirect.com
SCIENCE DIRECT®
International Journal of Heat and Mass Transfer 48 (2005) 3221–3230
International Journal of HEAT and MASS TRANSFER
www.elsevier.com/locate/ijhmt

Direct contact melting with asymmetric load

Hiroyuki Kumano *, Akio Saito, Seiji Okawa, Yuichi Yamada

Department of Mechanical Sciences and Engineering, Graduate School of Science and Engineering, Tokyo Institute of Technology, 2-12-1, Ookayama, Meguro-ku, Tokyo 152-8552, Japan

Received 21 August 2003; received in revised form 8 December 2004
Available online 27 April 2005

Abstract

In this study, direct contact melting with an asymmetric load was investigated both experimentally and by numerical analysis. A rectangular parallelepiped solid on a heating surface was melted under various asymmetric loads, while total load acting on the solid and brine temperature were kept constant. In the numerical analysis, the melting process keeping the force balance between the pressure in the liquid film and the loads at all times was calculated. It was found that the average heat flux into the solid was independent of the moment acting on the solid. Analytical results of the time dependencies of the amount of melting and the inclination of the solid agreed with experimental ones for each condition.

1. Introduction

In recent years, thermal energy storage systems have been attracting public attention as effective methods to preserve the environment, by promoting load leveling of electric power. Latent heat thermal energy storage is especially promising, since a high storage density can be obtained in comparison to the specific heat of the storage material. The melting process of the PCM (phase change material) progresses while the PCM solid is pressed against a heating plate due to gravity or buoyancy force, when there is a difference between the density of the liquid and the solid. In this case, melted liquid is squeezed out through a thin liquid film formed between the solid surface and the heating plate. Since heat is exchanged across this thin liquid film, a high heat flux can be obtained compared with a heat transfer that is, for example, dominated by natural convection. This phenomenon is known as direct contact melting and it is a very important phenomenon in determining the performance of a thermal energy storage system utilizing latent heat.

Over the past decade, many researchers have attempted to investigate the characteristics of direct contact melting [1–5]. The phenomenon of pressing a cylindrical solid onto a plate was first investigated experimentally and analytically by Saito et al. They showed a relationship between the heat flux, the Stefan number and the pressing force using non-dimensional parameters [1–3].

Many researchers, including those in the above studies, carried out their analyses by assuming that the force acts on the center of the PCM and that the melting process progresses symmetrically. When a realistic melting process in a thermal energy storage capsule is considered, an asymmetric condition must be considered.

In past studies, Hirata et al. [6] investigated direct contact melting under an asymmetric condition, both

* Corresponding author.
E-mail address: kumano@mech.titech.ac.jp (H. Kumano).

0017-9310/$ - see front matter © 2005 Elsevier Ltd. All rights reserved.
doi:10.1016/j.ijheatmasstransfer.2005.01.041

Nomenclature

Dimensional variables

c	specific heat, J/(kg K)
F^*	load acting on solid per unit length of depth, N/m
g^*	gravitational acceleration, m/s^2
h	heat transfer coefficient, W/(m^2 K)
H	height of solid, m
H_p	thickness of heating plate, m
L	latent heat of melting, J/kg
M^*	mass of solid per unit length of depth, kg/m
Mo^*	moment per unit length of depth, N
p^*	static gauge pressure, Pa
P^*	average pressure due to the gravitational force of the sample and the weight, Pa
q^*	heat flux, W/m^2
t^*	time, s
T	temperature, °C
T_{ref}	reference temperature, °C
U	flow rate per unit length of depth, m^2/s
u^*	velocity in x-direction, m/s
W^*	width of solid, m
W^*_{ini}	width of solid at initial condition, m
x^*, y^*	coordinates, m
x^*_p	position of maximum pressure, m

Greek symbols

α	thermal diffusivity, m^2/s
δ^*	thickness of liquid film, m
ΔT	temperature difference ($T_{ref} - T_m$)
λ	thermal conductivity, W/(m K)
μ	viscosity of liquid, Pa s
ρ	density, kg/m^3

Non-dimensional variables

c_1, c_2	coefficients
x_F	position of external force acting
x_R	position of resultant force acting
x_s	position of gravity center of solid

Subscripts

bot	bottom surface of the heating plate
f	medium
ini	initial condition
l	liquid
m	melting point
p	heating plate
surf	top surface of the heating plate

Definitions of non-dimensional variables

A_p	$= H_p/W^*_{ini}$
A_s	$= H/W^*_{ini}$
Bi	$= hW^*_{ini}/\lambda_l$
F	$= F^*W^*_{ini}/\mu\alpha_l$
g	$= g^*W^{*3}_{ini}/\alpha^2_l$
M	$= M^*\alpha_l/\mu W^{*2}_{ini}$
Mo	$= Mo^*/\mu\alpha_l$
P	$= P^*W^{*2}_{ini}/\mu\alpha_l$
p	$= p^*/p^*$
q	$= q^*W^*_{ini}/\lambda_l\Delta T$
Ste	$= c_l\Delta T/L$
t	$= t^*\alpha_l/W^{*2}_{ini}$
u	$= u^*\rho_l LW^*_{ini}/\lambda_l\Delta T$
W	$= W^*/W^*_{ini}$
x	$= x^*/W^*_{ini}$
y	$= y^*/W^*_{ini}$
δ	$= \delta^*/W^*_{ini}$
θ	$= (T - T_m)/\Delta T$

experimentally and analytically. They investigated the melting process of a solid leaning to one side at a constant temperature at the top of the heating plate. However, in a realistic melting process, various heating conditions must be considered.

Therefore, in this study, direct contact melting under an asymmetric load is investigated both experimentally and analytically. Experiments were carried out under various asymmetric loads, while the total load acting on the solid and the brine temperature were kept constant. In analysis, non-dimensional parameters were picked up through formulating non-dimensional governing equations. The calculations were carried out in order to understand the effects of changes in these parameters under three types of heating conditions—constant temperature at the top, constant heat flux at the bottom, and a constant heat transfer coefficient with constant temperature of the medium at the bottom of the heating plate.

2. Experimental

2.1. Experimental apparatus

For simplicity of the corresponding analysis, the PCM of a rectangular parallelepiped and a rectangular heating plate were used so that the flow in the thin liquid film could be treated conformably by two dimensional rectangular coordinates. Fig. 1 shows the main apparatus. The heating plate on which the direct contact melting occurred was a copper plate 240 mm in depth,

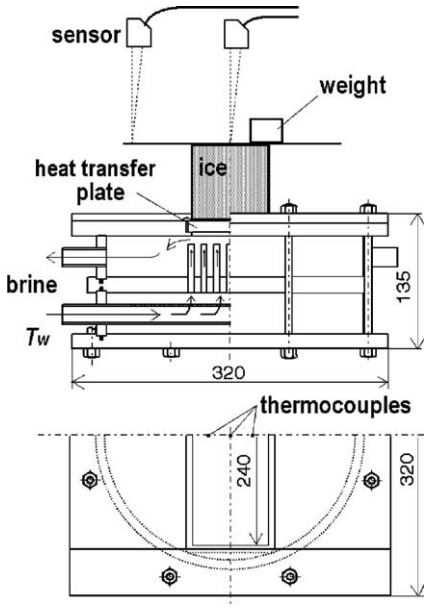

Fig. 1. Experimental apparatus.

80 mm in width and 10 mm in thickness. The surface temperature of the heating plate was adjusted by controlling the brine temperature blowing onto the bottom of the heating plate. The brine temperature was kept at a constant value throughout the experiment by using a constant temperature bath. The aspect ratio of the melting surface was decided in such a way that the melted liquid flowed in the width direction, and that the flow of the thin liquid film could be treated approximately with two dimensional rectangular coordinates. In a preliminary experiment, it was confirmed that the melted liquid flowed satisfactorily in the width direction. Six C–C thermocouples were installed in the heating plate, at the center and at locations 25 mm from the center. At each location, two thermocouples were installed at the points 2.75 mm from the top and the bottom of the heating plate, respectively. The temperature of the heating plate was measured by these thermocouples. The temperature distribution in the heating plate was assumed to be linear, and the surface and bottom temperatures were calculated from these measured values. A plastic plate was placed on the PCM to measure the change in the height of the solid at two points on the plate by two infrared displacement sensors. The amount of melting and the inclination of the PCM were calculated from the change in height.

A block of ice 80 mm in width, 240 mm in depth and 60 mm in height was used as the PCM. The ice was cut from transparent ice produced in such a way that it rarely included unfavorable air bubbles.

The PCM on the heating surface was melted under various asymmetric loads, while the weight acting on the PCM mentioned below and the brine temperature were kept at constant values for each experimental run. Time dependencies of the height and the inclination of the PCM were then measured, and the heat flux distribution and the amount of melting of the PCM were calculated. At the same time, the temperature in the heating plate was measured.

2.2. Experimental conditions

Experiments were carried out by varying the experimental conditions, that is, by varying the moment acting around the center of the solid and the brine temperature. The magnitude of the moment was adjusted by changing the position of the 0.464 kg weight, and the moment per unit length of depth around the center line was set at 0, 0.19, 0.38 or 0.57 N. The total load acting on the heat transfer surface is the summation of the load of the PCM, the load of the measurement plate and the load of the weight used to produce the moment. Since the total load and the moment changed with time due to the melting, these parameters were considered as the value at the initial state, and the initial total load per unit length of depth was set at 92.5 N/m. In addition, the brine temperature parameters were set at 4.8 and 10.6 °C.

3. Analysis

3.1. Governing equations

In the numerical analysis, the system was formulized in two-dimensional rectangular co-ordinates that were similar to the experimental conditions. Fig. 2 shows the co-ordinate system used for numerical analysis. The depth direction is perpendicular to the x–y plane. Governing equations were derived under the following assumptions:

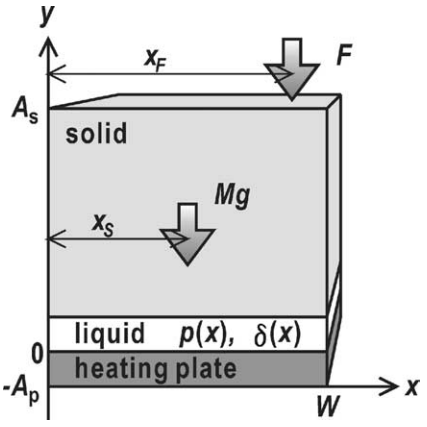

Fig. 2. Physical model.

(1) The momentum term in the flow is negligible.
(2) The pressure in the liquid film is uniform in the y-direction.
(3) The temperature in the solid PCM is uniform and kept at the melting point.
(4) The heat transfer in the liquid film is dominated by the heat conduction.
(5) The melting process is quasi-steady state.
(6) The heat flux is proportional to the distance along the width direction of the heating plate.
(7) The solid does not move in the x-direction.

In previous studies by the authors, the analytical solution obtained by using assumptions (1)–(5) agreed well with the experimental result for symmetric loading, if the *Ste* number was lower than 0.1. Therefore, assumptions (1)–(5) are considered appropriate. The move of the position of the resultant force in finite time difference can be neglected, and the variation in the thickness of the liquid film is very small compared with the motion of the PCM due to the melting. Then, the heat flux is proportional to the distance along the width direction of the heating plate, because the solid PCM inclines due to the melting. Therefore, assumption (6) is also appropriate, when the solid is in direct contact with the heating plate. Using the above assumptions, the calculations were carried out under three types of heating conditions, as follows:

Condition (1): Constant temperature at the top of the heating plate.
Condition (2): Constant heat flux at the bottom of the heating plate.
Condition (3): Constant heat transfer coefficient and constant temperature of the medium at the bottom of the heating plate.

Non-dimensional governing equations and boundary conditions based on the above assumptions are as follows:

Governing equations

$$\frac{\partial p}{\partial x} = \frac{Ste}{P}\frac{\partial^2 u}{\partial y^2} \tag{1}$$

$$\frac{\partial p}{\partial y} = 0 \tag{2}$$

$$Mg + F = P\int_0^W p(x)\,\mathrm{d}x \tag{3}$$

$$\int_0^W p(x)(x - x_\mathrm{R})\,\mathrm{d}x = 0 \tag{4}$$

$$\frac{\partial^2 \theta_\mathrm{p}}{\partial x^2} + \frac{\partial^2 \theta_\mathrm{p}}{\partial y^2} = 0 \tag{5}$$

The position of resultant force acting is expressed as follows:

$$x_\mathrm{R} = \frac{Fx_\mathrm{F} + Mgx_\mathrm{s}}{F + Mg} \tag{6}$$

Eqs. (1) and (2) are momentum equations in the liquid film, and Eqs. (3) and (4) show the force balance between the pressure in the liquid film and the load. Eq. (5) is the heat conduction equation of the heating plate. It was assumed that the melting process progresses in a quasi-steady state, keeping the force balance between the load and the pressure in the liquid film at every moment. Therefore, unsteady terms are not included in these equations, and the change in the mass of the PCM and the deviation of the center of gravity of the PCM in a finite time difference are neglected. Moreover, the heating plate temperature was calculated as steady state conduction, since it is considered that the temperature variation in the heating plate is very small.

When the heating condition investigated was that of constant temperature at the top of the heating plate, Eqs. (1)–(4) were used, and Eq. (5) was added to Eqs. (1)–(4) as the governing equations when the heating plate was included in the calculation region.

Boundary conditions are as follows for each heating condition:

Boundary conditions

Condition (1):

$$x = 0, W: \quad p = 0 \tag{7}$$

$$y = \delta: \quad u = 0,\ \theta_\mathrm{l} = 0 \tag{8}$$

$$y = 0: \quad u = 0,\ \theta_\mathrm{l} = 1 \tag{9}$$

Condition (2):

Eqs. (7), (8) and

$$x = 0, W \quad -A_\mathrm{p} \leqslant y \leqslant 0: \quad \frac{\partial \theta_\mathrm{p}}{\partial x} = 0 \tag{10}$$

$$y = 0: \quad u = 0,\ -\frac{\partial \theta_\mathrm{l}}{\partial y} = -\frac{\lambda_\mathrm{p}}{\lambda_\mathrm{l}}\frac{\partial \theta_\mathrm{p}}{\partial y} \tag{11}$$

$$y = -A_\mathrm{p}: \quad -\frac{\partial \theta_\mathrm{p}}{\partial y} = \frac{\lambda_\mathrm{l}}{\lambda_\mathrm{p}} q_\mathrm{bot} \tag{12}$$

Condition (3):

Eqs. (7), (8), (10), (11) and

$$y = -A_\mathrm{p}: \quad -\frac{\partial \theta_\mathrm{p}}{\partial y} = Bi\frac{\lambda_\mathrm{l}}{\lambda_\mathrm{p}}(\theta_\mathrm{f} - \theta_\mathrm{bot}) \tag{13}$$

The moment that is one of the parameters in the calculation varies with time due to the inclination of the solid and the movement of the center of gravity of the solid. Therefore, the value of the moment at the initial condition is given as the calculation parameter. The amount

of the moment at the initial condition is expressed as follows:

$$Mo_{\mathrm{ini}} = (F + M_{\mathrm{ini}}g)\left(x_{\mathrm{Rini}} - \frac{1}{2}\right) \tag{14}$$

The reference temperature to obtain the non-dimensional temperature is defined as the surface temperature of the heating plate. However, the surface temperature is not uniform when the asymmetrical load acts on the solid. It was found from past studies that the surface temperature is uniform when the load acts on the vertical line of the center of gravity of the solid. Therefore, the reference temperature is defined as the surface temperature when the moment is set to 0.

In this calculation, the melting process progresses in a quasi-steady state. However, the variation in the mass of the solid with melting and the moment generated by the change in the center of gravity of the solid must be considered. The mass and the position of the center of gravity of the solid at the next time step were calculated using the distribution of the heat flux through the liquid film, after obtaining a result that satisfied the governing equations. The heat flux through the liquid film is then expressed as follows, from assumptions (4) and (6):

$$q = \frac{\theta_{\mathrm{surf}} - \theta_{\mathrm{m}}}{\delta} = c_1 x + c_2 \tag{15}$$

The increase in the area of the melting surface, due to the inclination of the solid with melting, was also considered in the calculation. It was assumed that the load acted on the top of the solid. Therefore, it was considered that the position of the load varied with the inclination of the solid.

Using the above equations, the amount of melting, the mass of the solid and the variation of the center of gravity of the solid in finite difference time were obtained from the distribution of the heat flux at each time step. Moreover, the force balance was calculated using these values as the parameters at the next time step. The melting process was calculated by repeating these steps.

Time step was set to 1 s in the calculation for the comparison with the experimental results. In this study, the mass of the solid and the position of the resultant force vary with time due to the melting of the solid, and the calculation progresses to keep the force balance between the resultant force and the pressure in the liquid film in each time step. The variation of the mass of the solid is about 0.1%, and the variation of the position of the resultant force is about 0.02% of the width of the solid in 1 s. Therefore, these variations are sufficiently small to calculate the process continuously.

3.2. Numerical method for calculation of pressure

In this study, it is difficult to obtain pressure distributions in the liquid film and the thickness of the liquid film by numerical analysis, since the position of the load in the system is not symmetrical. The numerical method that was proposed by Nagakubo and Saito [7] is used to obtain the pressure distribution in the liquid film.

Following derivations are explicitly specified in dimensional forms. Eq. (1) is integrated twice, and velocity is derived by using Eqs. (8) and (9) as follows:

$$u^* = \frac{1}{2\mu}\frac{\partial p^*}{\partial x^*} y^* (y^* - \delta^*) \tag{16}$$

Flow rate is derived by integrating Eq. (16) with respect to the thickness of the liquid film.

$$U = \int_0^{\delta^*} u^* \,\mathrm{d}y^* = -\frac{1}{12\mu}\frac{\partial p^*}{\partial x^*}\delta^{*3} \tag{17}$$

Eqs. (16) and (17) can be treated as 2-dimensional Poiseuille flow. Moreover, the flow rate at a certain position is equal to the amount of melting at the region from a point of maximum pressure to the position under consideration. Assuming that heat transfer in the liquid film is dominated by heat conduction, the amount of the melting is expressed by the thickness of the liquid film and the surface temperature of the heating plate as follows:

$$U = \int_{x_{\mathrm{p}}^*}^{x^*} \lambda_{\mathrm{l}} \frac{(T_{\mathrm{surf}} - T_{\mathrm{m}})}{\delta^*} \frac{1}{L\rho_{\mathrm{l}}} \,\mathrm{d}x^* \tag{18}$$

The pressure gradient at a specific position is obtained from Eqs. (17) and (18) as follows:

$$\frac{\partial p^*}{\partial x^*} = -\frac{12\mu}{\delta^{*3}} \int_{x_{\mathrm{p}}^*}^{x^*} \lambda_{\mathrm{l}} \frac{(T_{\mathrm{surf}} - T_{\mathrm{m}})}{\delta^*} \frac{1}{L\rho_{\mathrm{l}}} \,\mathrm{d}x^* \tag{19}$$

First, two maximum pressure points are assumed near right and left side of the solid, and the pressure distributions between each maximum pressure point and each side of the solid are calculated by using Eqs. (7) and (19), respectively. Then, the values of the pressure at each maximum pressure point are compared, and the position having the lower value progresses to the inside. These procedures are repeated until obtaining coincidence of two maximum pressure points.

3.3. Parameters

The calculations were carried out with three types of heating conditions. Non-dimensional parameters were picked out from governing equations and boundary conditions. Table 1 shows non-dimensional parameters and the standard values of these at each condition. In this calculation, only a parameter of interest was varied, while other parameters were kept at the standard values. The effects on direct contact melting with an asymmetric load due to the change in this parameter were investigated. For the standard condition, it is taken that the heating plate is copper and the PCM solid is ice. The

Table 1
Parameters

Condition	(1)	(2)	(3)
P_{ini}		4.61×10^{10}	
$A_{s\,ini}$		1.0	
g		4.61×10^{11}	
M_{ini}		6.82×10^{-2}	
F		8.38×10^{9}	
Mo_{ini}		1.61×10^{9}	
Ste	0.051		
A_p			0.1
λ_p/λ_l			714
q_{bot}		977	
Bi			524
θ_f			3.0

width and height of the solid are 0.1 m, and the thickness of the heating plate is 0.01 m in the initial condition. P, A_s, M, Mo are decided by the mass of the solid and the load. Therefore, these values varied with melting, and the values of the initial condition in Table 1 were used as the calculation parameters.

In this study, the calculations were examined by varying the values of the moment, the surface temperature and the heat flux. In addition, the ratio of the thermal conductivity of the heating plate was varied.

4. Results and discussion

4.1. Comparison of experimental and analytical results

Experiments and numerical analyses were performed to confirm the validity of the analytical model. The heating conditions in the numerical analyses were set to a constant heat transfer coefficient and two different constant temperatures of medium at the bottom of the heating plate that were similar to the experimental conditions. The heat transfer coefficient at the bottom of the heating plate that was used in the numerical analysis was determined by preliminary experiments.

Fig. 3 shows the time dependency of the mass of the PCM and the inclination angle of the top of the PCM, at brine temperatures of 4.8 and 10.6 °C, respectively. The symbols show the experimental results for each condition, and the solid lines show the analytical results. The gradient of the change in the mass corresponds to the average heat flux for melting. It was found that the average heat flux for melting was independent of the moment acting on the solid, and that the heat flux was determined by the brine temperature and the total load, both experimentally and analytically. Moreover, it was found that the analytical results for the time dependency of the melting amount were independent of the moment, and coincided with the experimental results for each condition.

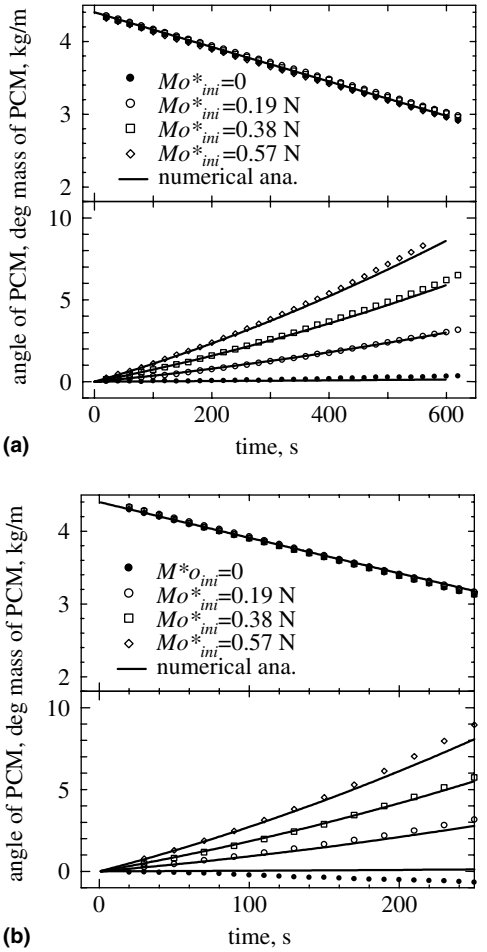

Fig. 3. Time dependency of mass and angle of PCM solid: (a) T_f = 4.8 °C and (b) T_f = 10.6 °C.

As the moment increased, the inclination of the PCM became larger with time. It is supposed that the liquid film becomes thinner on the side the moment acts on, in order to keep the force balance between the pressure in the liquid film and the loads. Therefore, the heat flux increases on this side, because the effect of thermal resistance decreases. In the experiment, it was observed that the surface temperature of the side the moment was acting on was lower than the temperature of the other side, though the amount of melting was larger on that side. Therefore, it was found that the effect of decreasing the thickness of the liquid film was more significant than the effect of decreasing the surface temperature.

The experimental results coincided with the analytical ones for all conditions. Therefore, it was concluded that the analytical model is reasonable. In this calculation, the mass of the solid and the position of the resultant force vary with time due to the melting of the solid. Thus, the variation of the center of gravity of the solid

and the mass of the solid can be obtained accurately for the whole melting process, since the heat flux distribution can be calculated accurately in each time step.

4.2. Analytical results

In this study, the parameters that dominate the melting process under each heating condition were picked out, and the effects of changing several parameters were examined for each condition.

4.2.1. Constant temperature at the top of the heating plate

Fig. 4 shows the analytical result for the melting process under condition (1), that is, constant temperature at the top of the heating plate. The parameters were set at the values in Table 1. The load acted on the top at the right side of the solid, and it was found that the melting process progressed as the solid inclined to the right side.

Fig. 5 shows the time dependency of the mass of the solid and the inclination angle of the solid, when the moment was varied. The other parameters were set at the values in Table 1.

The mass of the solid and the time are non-dimensional values. It was found that the amount of melting was independent of the moment, and this tendency was similar to that found in the experimental results.

Fig. 6 shows the time dependency of the mass and the inclination angle of the PCM, when *Ste* was varied. As *Ste* increased, the change in the mass of the PCM increased, and this result corresponds to a finding of previous studies that the heat flux is determined by *Ste*. However, the effect of *Ste* on the distribution of the heat flux is not clear in Fig. 6, since the mass of the PCM under each condition is different when the same amount of time has passed. Therefore, the relationship between the mass and the inclination angle of the PCM is shown in Fig. 7. It is found that these relationships correspond to each other despite the difference in *Ste*, and a locus of the solid on the melting process is the same when the moment is set to the same initial value.

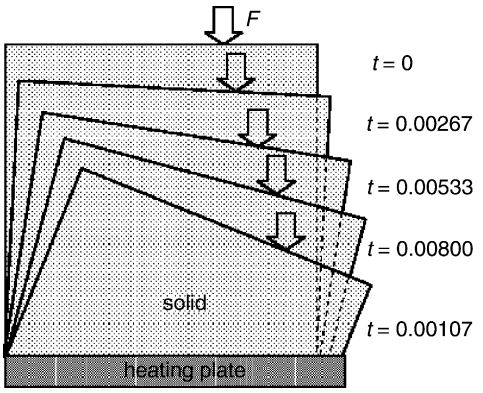

Fig. 4. Melting process of PCM solid for condition (1).

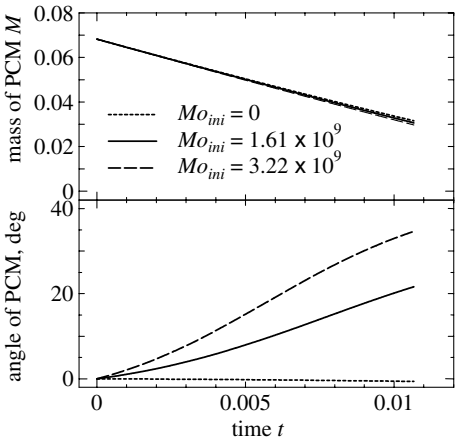

Fig. 5. Effects of Mo_{ini} for condition (1).

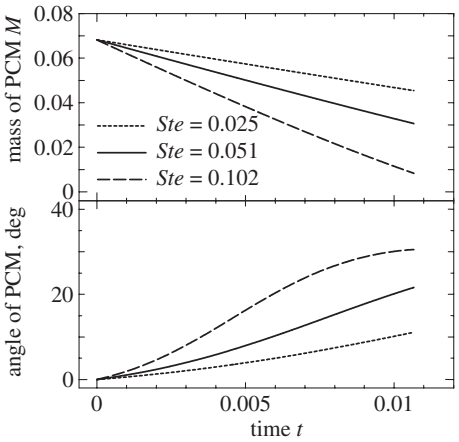

Fig. 6. Effects of *Ste* for condition (1).

4.2.2. Constant heat flux at the bottom of the heating plate

Fig. 8 shows the time dependency of the mass of the solid and the inclination angle of the solid when the moment is changed. Since the heat flux at the bottom of the heating plate is constant, the variations in the mass of the solid agree with each condition. The inclination angle increases with the moment, but the angle is small compared with condition (1). It is supposed that the inclination angle of the solid depends on heating plate properties, and that heat transfer in the heating plate is significant in the melting process.

Fig. 9 shows the time dependency of the mass of the solid and the inclination angle of solid, when the ratio of the thermal conductivity of the heating plate to that of

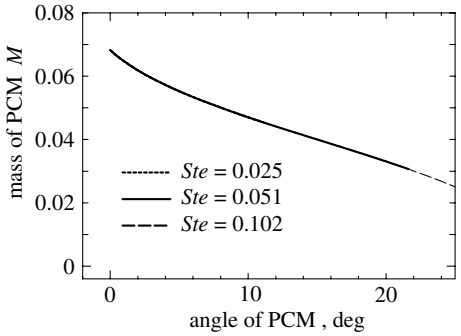

Fig. 7. Relationship between angle and mass of solid.

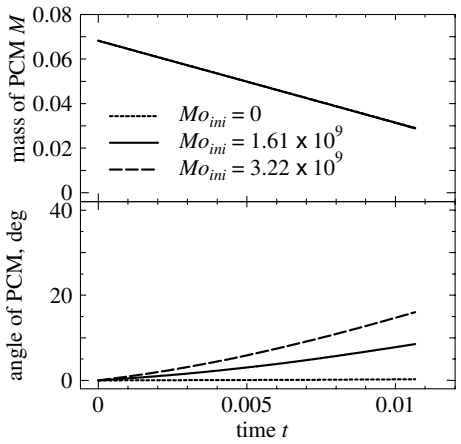

Fig. 8. Effects of Mo_{ini} for condition (2).

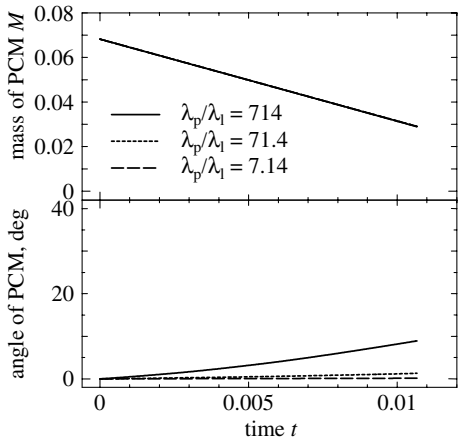

Fig. 9. Effects of λ_p/λ_l for condition (2).

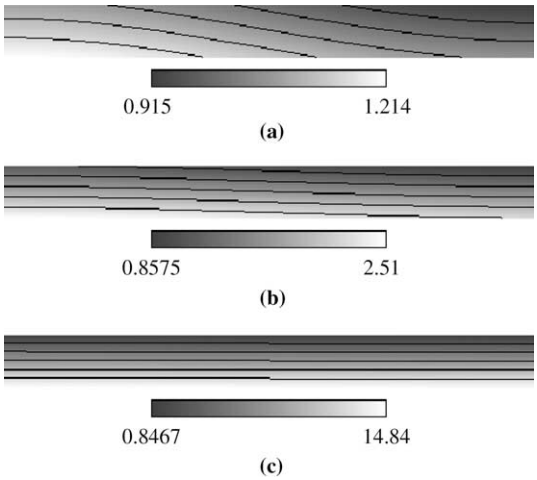

Fig. 10. Temperature distribution in the heating plate: (a) $\lambda_p/\lambda_l = 714$, (b) $\lambda_p/\lambda_l = 71.4$ and (c) $\lambda_p/\lambda_l = 7.14$.

the liquid is changed. The moment was set to the same initial value. It was found that the inclination angle of the solid became larger with an increase in the thermal conductivity of the heating plate. Moreover, the temperature distribution in the heating plate at $t = 0$ is shown to reveal the effect of the thermal conductivity of the heating plate, when the ratio is varied (Fig. 10). The load acts on the right side of the solid in the figures, and the solid lines show contour lines of the non-dimensional temperature. It can be seen in Fig. 10 that the heat flow in the x-direction increases as the thermal conductivity of the heating plate increases. Therefore, the inclination angle of the solid is dominated by the thermal conductivity of the heating plate under this condition.

4.2.3. Constant heat transfer coefficient and constant medium temperature at the bottom of the heating plate

Fig. 11 shows the time dependency of the mass of the solid and the inclination angle of the solid when the moment is changed. The inclination angle of the solid becomes larger as compared to condition (2), because the heat flux distribution exists at the bottom surface of the heating plate in the case of condition (3).

Fig. 12 shows the time dependency of the mass of the solid and the inclination angle of the solid when the ratio of the thermal conductivity of liquid to that of the heating plate is changed and the moment is set to the same initial value. The heat flux decreases with decreasing thermal conductivity in the heating plate, due to the change in the thermal resistance between the bottom of the heating plate and the solid. However, in this case, it is difficult to compare the effect of the thermal conductivity on the inclination angle of the solid in Fig. 12, because the amount of melting differs at the same time points. Thus, the relationship between the mass and the inclination angle of the PCM is shown in Fig. 13. It is found that the inclination angle increases with an increase in the ratio of the thermal conductivity, and this tendency is similar to the results obtained for condition

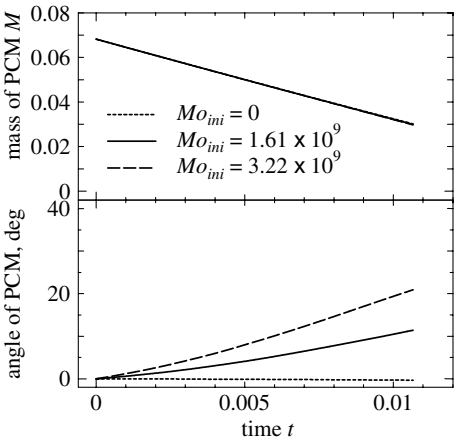

Fig. 11. Effects of Mo_{ini} for condition (3).

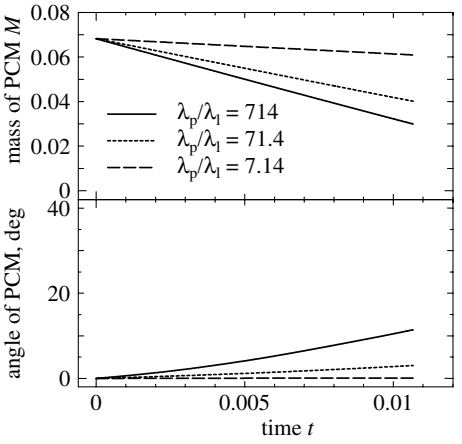

Fig. 12. Effects of λ_p/λ_l for condition (3).

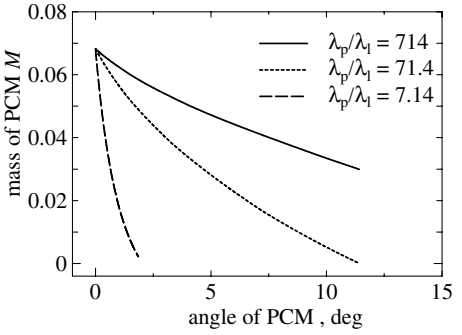

Fig. 13. Relationship between angle and mass of solid.

(2). When the thermal conductivity of the heating plate is large, the heat flux distribution becomes larger, since the temperature at the bottom of the heating plate becomes smaller at the side the load acts on. Therefore, the increase in the inclination angle is caused by this effect, in addition to an effect of heat flow in the y-direction.

5. Conclusion

Direct contact melting with an asymmetric load was investigated both experimentally and by numerical analysis. It was found that the average heat flux into the PCM was independent of the moment acting on the solid, but was determined by the total load and the brine temperature, both experimentally and analytically. The analytical results for the time dependency of the amount of melting and the inclination angle of the PCM agreed with the experimental results. Three types of heating conditions were examined by numerical analysis, and the parameters that dominated the phenomenon under each condition were picked out. The effects of changing several parameters were investigated from the points of view of the average heat flux and the inclination of the solid. As a result, it was found that a locus of the solid on the melting process is the same despite the difference in *Ste*, when the moment is set to the same initial value, in the constant temperature condition at the top of the heating plate. Moreover, it was found that the inclination angle of the solid became larger with an increase in the thermal conductivity of the heating plate in the heating condition at the bottom of the heating plate.

Acknowledgements

The authors acknowledge the financial support of the Japan Society for the Promotion of Science under the project name of Research for the Future (JSPS-RFTF 97P01003, Fundamental Research on Thermal Energy Storage to Preserve Environment).

References

[1] A. Saito, Y. Utaka, M. Akiyoshi, K. Katayama, On the contact heat transfer with melting (1st report), Bull. JSME 28 (240) (1985) 1142–1149.

[2] A. Saito, Y. Utaka, M. Akiyoshi, K. Katayama, On the contact heat transfer with melting (2nd report), Bull. JSME 28 (242) (1985) 1703–1709.

[3] A. Saito, Y. Utaka, K. Shinoda, K. Katayama, Basic research on the latent heat thermal energy storage utilizing the contact melting phenomena, Bull. JSME 29 (255) (1986) 2946–2952.

[4] M. Bareiss, H. Beer, An analytical solution of the heat transfer process during melting of an unfixed solid phase change material inside a horizontal tube, Int. J. Heat Mass Transfer 27 (1984) 739–745.

[5] M.K. Moallemi, B.W. Webb, R. Viskanta, An experimental and analytical study of close-contact melting, ASME, J. Heat Transfer 108 (1986) 894–899.
[6] T. Hirata, M. Ishikawa, R. Hashimoto, Direct contact melting of two-dimensional arbitrarily shaped solids on an isothermally heated horizontal plate, Heat Transfer Jap. Res. 24 (7) (1995) 589–602.
[7] S. Nagakubo, A. Saito, Numerical analysis on a direct contact melting process, Trans. JAR 4 (3) (1987) 37–45 (in Japanese).